Nuclear Inst. and Methods in Physics Research, A 871 (2017) 113–117

Contents lists available at ScienceDirect

Nuclear Inst. and Methods in Physics Research, A

journal homepage: www.elsevier.com/locate/nima

Performance study of a large 1 × 1 m^2 MRPC with 1 × 1 cm^2 readout pads

F. Carnesecchi [a,b], C. Combaret [c], I. Laktineh [c], Z. Liu [d,e,*], L. Mirabito [c], D.W. Kim [d,e], O.M. Rodriguez [d,g], W. Park [d,e], S. Vallecorsa [e], M.C.S. Williams [b,f], A. Zichichi [a,b,f], R. Zuyeuski [a,d]

[a] Museo Storico della Fisica e Centro Studi e Ricerche E. Fermi, Roma, Italy
[b] INFN and Dipartimento di Fisica e Astronomia, Universit di Bologna, Italy
[c] Univ. Lyon, Université Lyon 1, CNRS/IN2P3, IPNL4 rue E Fermi 69622, Villeurbanne CEDEX, France
[d] ICSC World Laboratory, Geneva, Switzerland
[e] Gangneung-Wonju National University, Gangneung, South Korea
[f] European Centre for Nuclear Research (CERN), Geneva, Switzerland
[g] University Hermanoz Saiz, Pinar del Rio, Cuba

ARTICLE INFO

Keywords:
Multigap resistive plate chamber
Fishing lines
Efficiency
Dark count rate
Multiplicity

ABSTRACT

A Semi-Digital Hadronic Calorimeter (SDHCAL) concept has been proposed for future leptonic collider experiments. The multigap resistive plate chamber (MRPC) is a candidate for the detector planes of this calorimeter. We have constructed three MRPCs of 1m × 1m size for tests of the SDHCAL. Two have 4 gas gaps and one has 5 gas gaps. To achieve high granularity for a calorimeter, the signals from the MRPC are readout by $1\times1\ cm^2$ pads. The three MRPCs have similar design but the fishing line spacer has different configurations. All three MRPCs were successfully tested in the T10 test beam facility at CERN with a gas mixture of 95% $C_2H_2F_4$ and 5% SF_6. The efficiency and multiplicity of these chambers have been studied. All chamber reached around 94% efficiency at the proper operating voltage.

1. Introduction

The multigap resistive plate chamber (MRPC) has been developed for the ALICE Time of Flight (TOF) due to its very good timing capabilities [1]. Typically the MRPC has a time resolution better than 100 ps [2]. The excellent timing performance, the reasonable cost for large area production and the low noise level makes it widely used in high energy physics experiments. The TOF information provided by the MRPC can be used for the identification of the charged particles or to time log different events happening in a short time period. A Semi-Digital Hadronic Calorimeter (SDHCAL) concept has been proposed for future leptonic collider experiments [3]. Such detectors should have high granularity, high efficiency, compactness and low power consumption [4]. The SDHCAL consists of 49 iron plates (1.5 cm thickness) with 48 gaps (13 mm) between the iron plates [5]. A cassette (1 × 1 m^2 area and 10.9 mm width) containing the detector and the electronics can be slid into this gap; a cross section of the cassette is shown in Fig. 1. Because of the compact design of the cassette, the thickness of the MRPC is limited to about 2.8 mm. A 1 × 1 cm^2 segmentation for SDHCAL is a good compromise with respect to cost and number of readout channels. We have built three very thin large area MRPCs with single-ended 1 × 1 cm^2 pad readout to check if their performance meets the requirements of SDHCAL. Here we present the beam test results of our MRPC prototypes with a dimension of 1 × 1 m^2, which show that the MRPCs can be used as the SDHCAL detector planes.

2. 1 × 1 m^2 multigap resistive plate chamber

In ALICE-TOF the induced signals on the pick-up strips of the MRPCs are read out differentially by NINO ASIC [6]. However, to achieve high granularity in a calorimeter, the 1 × 1 m^2 area MRPC prototype has 1 × 1 cm^2 pick up pads over the surface; thus a differential readout is not practical. For our prototypes, groups of 64 pads are connected to a HARDROC ASIC [7].

Three MRPCs were constructed: two (MRPC1 and MRPC2) have 4 gas gaps, while MRPC3 has 5 gaps. The detectors are similar except that they have different fishing line configuration. Fig. 1 shows the cross section of an edge of the chamber. Two 400 μm thickness glass sheets with a dimension of 100×100 cm^2 are used for the outer glass plates. The three inner glass sheets have a thickness of 280 μm and a size of 99.5×97.7 cm^2. A 300 μm gas gap between each glass sheet is created by fishing line

* Correspondence to: PH department, CERN, Geneva, Switzerland.
E-mail address: zheng.liu@cern.ch (Z. Liu).

http://dx.doi.org/10.1016/j.nima.2017.07.068
Received 5 April 2017; Received in revised form 23 June 2017; Accepted 31 July 2017
Available online 5 August 2017

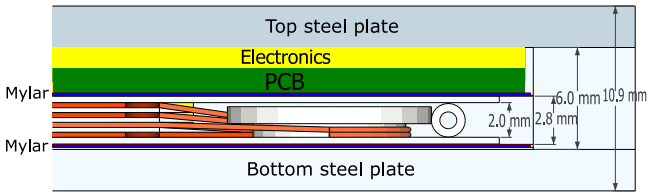

Fig. 1. Cross section of the 4 gaps MRPC.

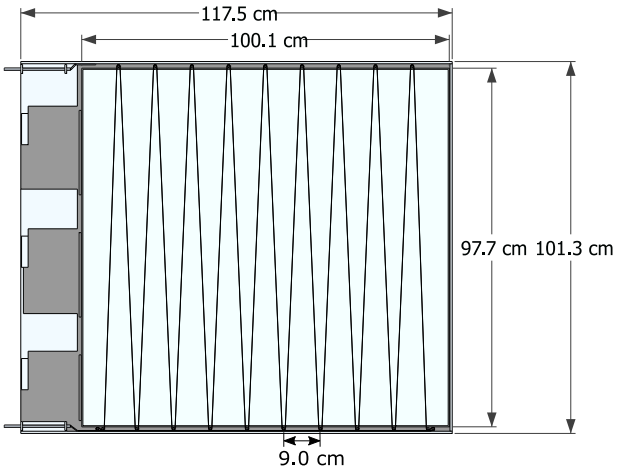

Fig. 2. Schematic of fishing line configuration of MRPC1.

spacers. These fishing lines are fixed along the sides by Teflon washers. The outside surfaces of the two outer glass sheets were coated with resistive paint to form the anode and the cathode respectively. A mylar sheet covers and isolates these voltage layers. The lower coated glass is the cathode and connected to negative high voltage. The top coated glass is the anode and connected to the ground of the high voltage supply. A printed circuit board (PCB) containing front-end electronics and pick up pads was placed on the top of the chamber. The pads are etched on one side of the PCB with a size of 1×1 cm^2. A gap of 0.406 mm separates two neighbouring pads. The pick-up signal from the pads is sent to the input of the HARDROC chips on the other side of PCB by a transmission line. The transmission line is created by the trace and the ground plane of the PCB. The ground plane is well connected to the metal plates of the cassette since these serve as the cathode pick-up electrode. The two external stainless steel plates were placed on each side of the chamber to support the glass and electronics. The total thickness of the detector, including the electronics and the metal plates, is 10.9 mm. The cross section of MRPC3 is similar to MRPC1 except that it has 5 gas gaps. Due to the constraints of the total thickness of the MRPC, the gas gap of MRPC3 was reduced to 250 μm and one of the outer glass plates has a thickness of 280 μm. (The other remains at 400 μm.)

Fig. 2 shows a schematic diagram of the fishing line configuration for MRPC1, which has an active area of 98.2×96.2 cm^2. 10 Teflon washers are glued along one side and 9 washers are glued along the other side. The distance between two washers is 9.0 cm. A fishing line crosses the glass sheets and goes around the Teflon washers as shown in Fig. 2. Fig. 3 is a picture of MRPC1, which clearly shows the form of the fishing line. MRPC2 has the same active area as MRPC1 but a different fishing line configuration as shown in Fig. 4. The Teflon washers were symmetrically placed along both sides. A schematic of the fishing line configuration for two layers is shown in Fig. 5. For the odd number layers, the fishing line (blue) crosses from washer D to washer A and washer E then washer C, the washer B between A and C is not used for these layers. In the even number layer of gas gap, the fishing line (red) crosses from washer F to washer B then to washer D.

Fig. 3. Picture of the MRPC1.

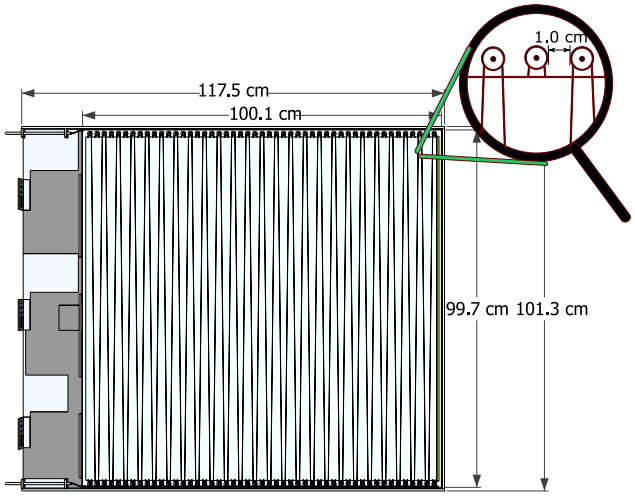

Fig. 4. Schematic of fishing line configuration of MRPC2. Only one layer of fishing line is shown. Right corner of the top is zoom in.

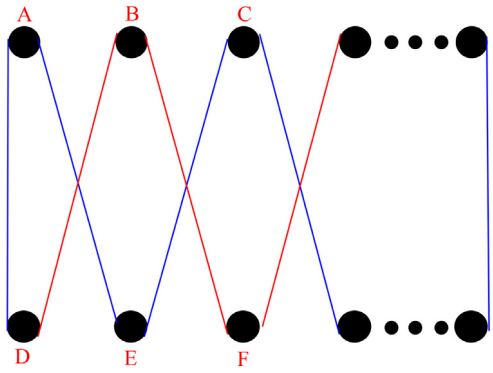

Fig. 5. Schematic of the fishing configuration for odd and even number layers in MRPC2. The dimensions are not scaled. (For interpretation of the references to colour in this figure legend, the reader is referred to the web version of this article.)

The layout of the fishing line for MRPC3 is a series of parallel crossings, however the direction is orthogonal between even and odd gas gaps. This is shown in Fig. 6. The Teflon washers are grouped as pairs and placed on 4 sides of the chamber. The width of a Teflon washer group is 2.4 cm and the distance between two groups is 1.9 cm. The fishing line (blue) in the odd number layers crosses the glass sheet orthogonal to the fishing line (red) in the even number layers. The fishing line can be clearly seen in the photo shown in Fig. 7.

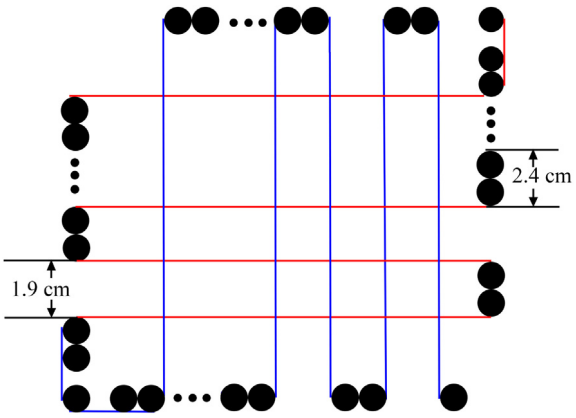

Fig. 6. Schematic of the fishing configuration for odd and even number layers in MRPC3. The dimension is not scaled. (For interpretation of the references to colour in this figure legend, the reader is referred to the web version of this article.)

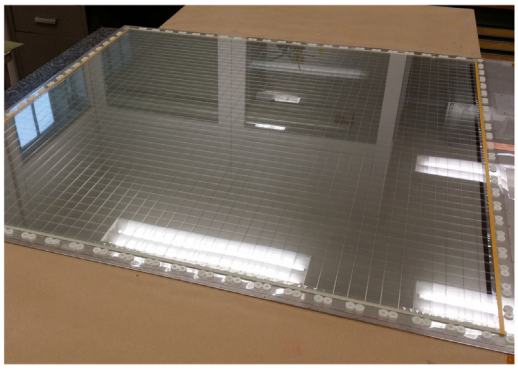

Fig. 7. Picture of the MRPC3.

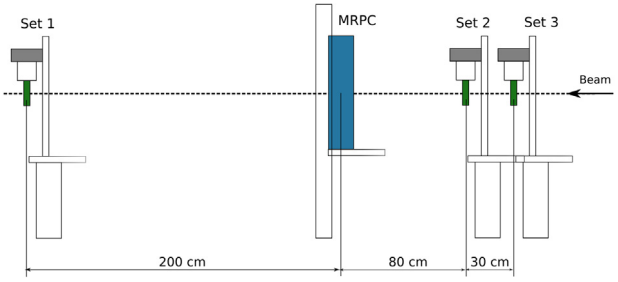

Fig. 8. The experimental setup in T10 test beam facility.

3. Experimental setup

The MRPCs were tested in T10 test beam facility at CERN. Fig. 8 shows a sketch of the experimental setup. The beam (mostly negative pions of 5 GeV/c momentum) has a direction perpendicular to the chamber. A gas mixture of 95% $C_2H_2F_4$ and 5% SF_6 was flowed through the chambers at a rate of 5 l/h. Three sets of crossed scintillators coupled to photomultiplier tubes (PMTs) were used to select a small (1×1 cm^2) area of the beam and to provide the trigger signal. All scintillators were well aligned with respect to the beam line. The data was read out by a DAQ PC via a USB cable communication. The MRPCs were mounted on a X–Y moving stage with precision of 1 mm, which could be controlled remotely. To centralize the beam spot to the readout pad, a position scan with 1 mm step was performed.

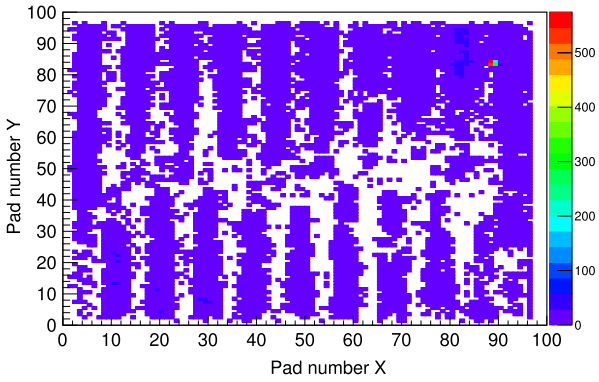

Fig. 9. 2D hit map of MRPC1 in the test beam including the noise. The threshold was set at 114 fC. The measurement was with an 12 kV.

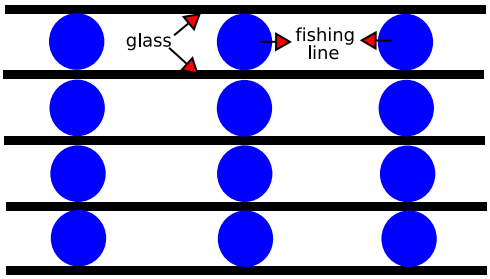

Fig. 10. Schematic of glass sheet shape in a normal MRPC. Black line is lines represent the glasses and blue circle is circles represent the fishing lines. (For interpretation of the references to colour in this figure legend, the reader is referred to the web version of this article.)

4. Results and discussion

4.1. 4 gas gaps MRPC

The 2D hit map of MRPC1 is shown in Fig. 9. A hit was recorded if the induced signal passed the threshold of HARDROC ASIC. The x, y coordinates and time-stamp of the hit were registered. The bin size in the HARDROC is 200 ns, which is defined by the 5 MHz clock. The total live time of the HARDROC is 20 ms; for the efficiency and multiplicity studies we apply a cut at time bin 10, thus selecting a 2 μs window in time with the through-going beam particle. We investigated noise hits by looking at hits with times earlier than 20 μs. A pattern within the noise map can be clearly seen in Fig. 9. Examining Figs. 2 and 9, it is not hard to find that this pattern is related to the fishing line configuration of MRPC1. In the ideal case of the MRPC the glass sheet is flat and well supported by the fishing line. However, the glass sheets can be distorted due to insufficient support of the fishing lines when high voltage is applied. Displacement of the glass sheet will increase the electric field in some regions and will thus increase the noise rate. Figs. 10 and 11 are the schematic drawings of glass shape in the ideal case and in the case where the glass sheets have been distorted, respectively. MRPC2 was built with an increased number of the fishing lines. As can be seen in Fig. 12, the noise is quite homogeneous and no pattern as seen in Fig. 9 was found.

The noise levels at different voltages for two MRPCs are shown in Figs. 13 and 14. As shown in Fig. 13, the dark count rate (DCR) of MRPC1 was quite high compared with the normal noise level ($\leq$ 2.7 Hz/cm^2 at room temperature when the electric field strength in the gas gap is close to 100 kV/cm [8]). The DCR was about 20 Hz/cm^2 at 10 kV and it increased to 80 Hz/cm^2 at 12 kV (E = 100 kV/cm). However, by changing the fishing line configuration in MRPC2, we achieved a lower noise level as shown in Fig. 14. The noise rate was about 1.1 Hz/cm^2 at 12 kV.

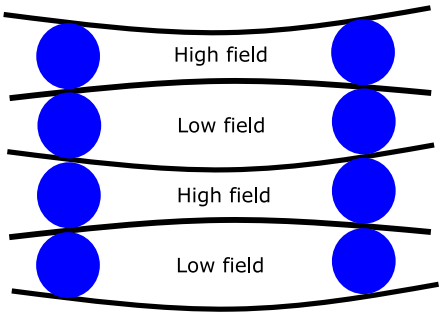

Fig. 11. Distortion of glass sheet shape due to the high electric field in the gaps.

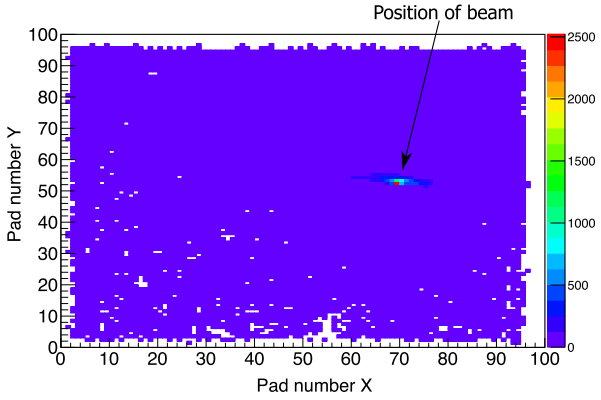

Fig. 12. 2D hit map of MRPC2 in the test beam including the noise. The threshold was set at 114 fC. The measurement was performed with an applied voltage of 12 kV.

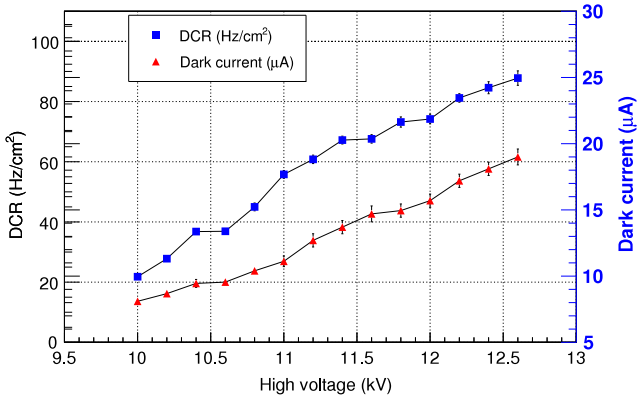

Fig. 13. The noise level of MRPC1 as a function of the applied high voltage, at a threshold of 114 fC.

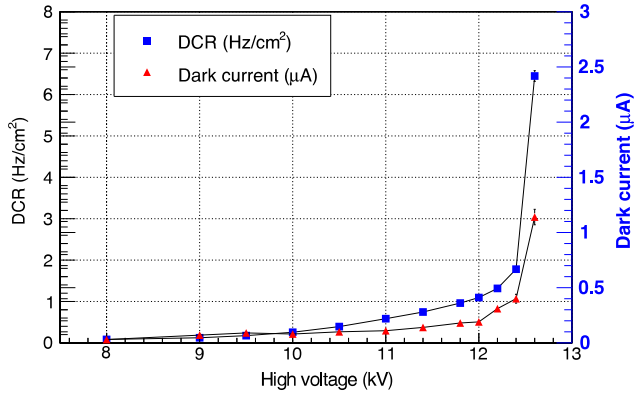

Fig. 14. The noise level of MRPC2 at a threshold of 114 fC.

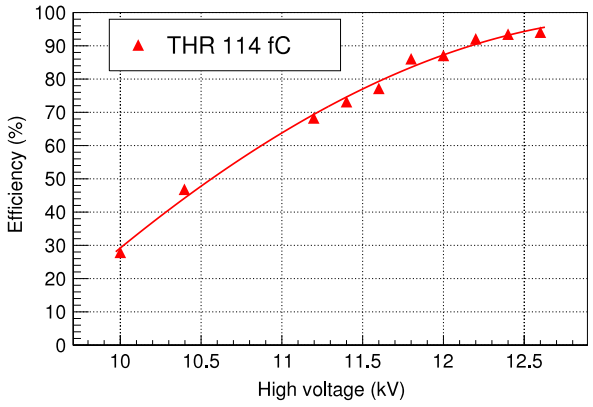

Fig. 15. The efficiency of MRPC1 as a function of the applied high voltage.

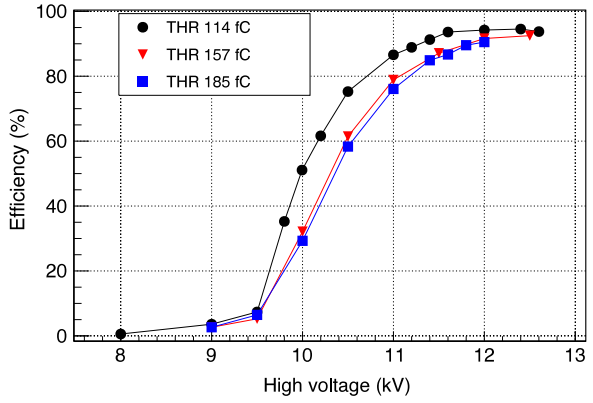

Fig. 16. The efficiency MRPC2 as a function of the applied high voltage. Three different thresholds are applied.

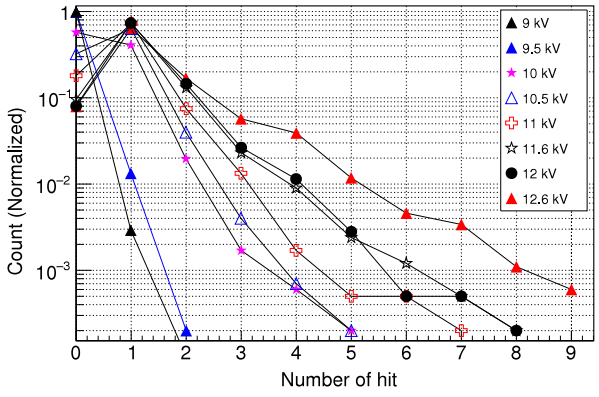

Fig. 17. The multiplicity plot of the MRPC2. All measurements were performed with a threshold set at 114 fC.

Fig. 15 shows the efficiency of MRPC1 as a function of high voltage. The efficiency of MRPC1 reached 94% at 12.5 kV. The efficiency plot of MRPC2 is given in Fig. 16. The efficiency is measured at three different thresholds. When the voltage is higher than 12 kV, the efficiency enters a plateau with a value of 94%–95%. The trend of efficiency as a function of voltage is similar in three threshold settings with the highest efficiency decreasing with increasing threshold.

A plot of the multiplicity distribution for MRPC2 is shown in Fig. 17. The mean value of the number of hits increases with higher voltage. At the voltage of 12 kV (94% efficiency), 75% of the events record a single hit. The idea of SDHCAL is to count the number of tracks in each sample

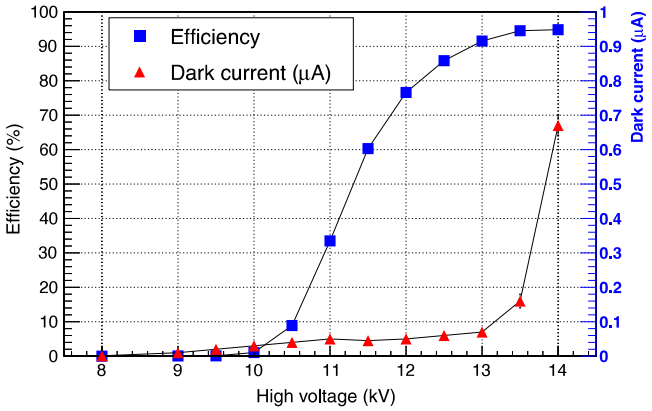

Fig. 18. The efficiency and dark current as a function at different voltages of MRPC3. The threshold was set at 114 fC.

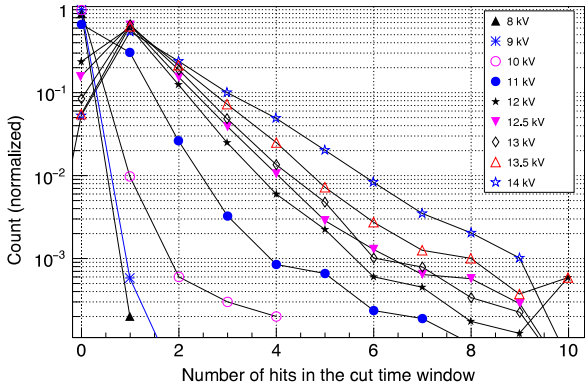

Fig. 19. The multiplicity plot of the MRPC3. The threshold was set at 114 fC.

and relate this to the energy deposit; and thus it is better to have a large fraction of single hits.

4.2. 5 gas gaps MRPC

As we expected, there was no fishing line pattern in the 2D hit map of MRPC3 since the glass sheets are supported by orthogonal lines of fishing lines in alternate gaps. The efficiency and dark current of MRPC3 at different operating voltages are shown together in Fig. 18. The efficiency reached 94.5% at 13.5 kV with a low dark current of 0.15 μ A/m^2. The efficiency plateau of MRPC3 starts at a higher applied voltage since the total gas gap size is larger (1.25 mm compared with the 1.2 mm of MRPC1 and MRPC2). Fig. 19 shows the multiplicity distribution of MRPC3, which is similar to that of MRPC2. However, at the voltage of 13.5 kV (94.5% efficiency), 62.5% of the events registered single hit.

5. Conclusion

We have successfully operated the 1 × 1 m^2 MRPCs with 96 ×96 1 × 1 cm^2 pick up pads. MRPC1 had substantially larger noise rates due to insufficient fishing line; a noise pattern that matched the fishing line configuration was found. Increasing the fishing line, and changing the pattern reduces the noise rate and eliminated the noise pattern observed in the MRPC. The efficiency of these three MRPCs all reached to 94%. The time performance has not been evaluated in current prototypes. We will start to develop another prototype of MRPC with using an ASIC chips that can perform sub ns timing measurements.

Acknowledgements

This work has been supported by the Korea-EU cooperation programme of National Research Foundation of Korea, Grant Agreement 2014K1A3A7A03075053. The results presented here were obtained at the T10 test beam in the east hall at CERN. The authors acknowledge the support received by the operators of the PS. The authors also thank to Prof. Imad Laktineh group from University Lyon for the technical support.

References

[1] A.N. Akindinov, et al., Latest results on the performance of the multigap resistive plate chamber used for the ALICE TOF, Nucl. Instrum. Methods Phys. Res., Sect. A 533 (1) (2004) 74–78.
[2] A. Akindinov, et al., The multigap resistive plate chamber as a time-of-flight detector, Nucl. Instrum. Methods Phys. Res., Sect. A 456 (1) (2000) 16–22.
[3] G. Baulieu, et al., Construction and commissioning of a technological prototype of a high-granularity semi-digital hadronic calorimeter, J. Instrum. 10 (10) (2015) P10039.
[4] Arnaud Steen, CALICE collaboration, Results of the CALICE SDHCAL technological prototype, J. Phys. Conf. Ser. 587 (1) (2015) IOP Publishing.
[5] CALICE collaboration, First results of the CALICE SDHCAL technological prototype, J. Instrum. 11 (04) (2016) P04001.
[6] F. Anghinolfi, et al., NINO: an ultra-fast and low-power front-end amplifier/discriminator ASIC designed for the multigap resistive plate chamber, Nucl. Instrum. Methods Phys. Res., Sect. A 533 (1) (2004) 183–187.
[7] Frederic Dulucq, et al., HARDROC: Readout chip for CALICE/EUDET digital hadronic calorimeter, in: Nuclear Science Symposium Conference Record (NSS/MIC), 2010 IEEE, IEEE, 2010.
[8] Tao Zou, et al., Quality control of MRPC mass production for STAR TOF, Nucl. Instrum. Methods Phys. Res., Sect. A 605 (3) (2009) 282–292.